Journal of Porphyrins and Phthalocyanines
J. Porphyrins Phthalocyanines 2021; 937–943
DOI: 10.1142/S1088424621500553

Published at https://www.worldscinet.com/jpp/

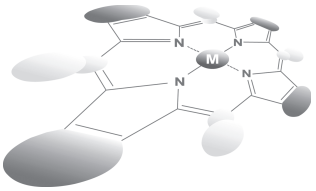

Synthesis, properties and reactivity of an *ortho*-phenylene-cyclopentene-bridged tetrapyrrole

Yuki Morimoto, Atsuhiro Osuka and Takayuki Tanaka*◊

Department of Chemistry, Graduate School of Science, Kyoto University, Kitashirakawa Oiwake-cho, Sakyo-ku, Kyoto 606-8502, Japan

Received 31 March 2021
Accepted 12 April 2021

Dedicated to Professors Lechosław Latos-Grażyński and Hiroyuki Furuta on the occasion of their 70th and 65th birthdays, respectively

ABSTRACT: Increasing the number of *meso*-methine carbons of porphyrin has led to a creation of a series of vinylogous expanded porphyrins, while the introduction of an *ortho*-phenylene-unit as a pyrrole-connecting two-carbon bridge usually leads to prevention of effective macrocyclic conjugation. Cyclopentene can serve as a conjugative bridge to increase the macrocyclic conjugation owing to its *cis*-geometry. In this work, *ortho*-phenylene-cyclopentene-bridged tetrapyrrole **5** was prepared on the basis of a coupling strategy. The tetrapyrrole **5** exhibited slightly more conjugative features as compared to *ortho*-phenylene-bridged tetrapyrrole **4**. Oxidation of **5** with [bis(trifluoroacetoxy)iodo]benzene (PIFA) at low temperature afforded a partly fused tetrapyrrolic compound **9** having a spiro-connected pyrrolo[2,1-*a*]isoindole moiety.

KEYWORDS: cyclopentene, coupling reaction, emission, oxidative fusion reaction.

INTRODUCTION

Usual porphyrins contain one *meso*-methine carbon between two pyrrole units. An increase in the number of bridging carbons affords various vinylogous porphyrins with variable aromatic characters. The synthesis of such vinylogous porphyrins was extensively examined more than three decades ago [1]. On the other hand, porphycenes, *i.e.* porphyrins(2.0.2.0), are intriguing isomeric porphyrins mainly due to their bathochromically shifted absorption bands due to the lack of degeneracy in their LUMOs [3]. These attributes stem from effective conjugation between the two bipyrrole units in which the bridging of two ethene moieties take on a *cis*-geometry. On the contrary, porphyrin(2.1.2.1) and porphyrin(2.2.2.2) are known to take on both *cis*- and *trans*-ethene configurations in order to acquire effective intramolecular hydrogen-bonding interaction [4, 5]. Among them, the synthesis of β-octaethylporphyrin(2.2.2.2) was first reported in 1990, and has recently been reinvestigated [5, 6]. The structure of porphyrin(2.2.2.2) with all-*cis* form (**1**) has never been identified. Instead, a planar oxidized form (**2**) with a *cis-trans-cis-trans* ethene configuration was isolated as a stable form and characterized as a 22π aromatic molecule. Different from a flexible ethene bridge, *ortho*-phenylene can serve as a rigid two-carbon bridge with a defined *cis*-geometry. The effects of the phenylene-type bridges have been systematically studied in the triphyrin(2.1.1) system such as **3** [7]. In 2015, tetrapyrrole **4** with four *ortho*-phenylene bridges was synthesized by our group and showed fairly less-conjugative features relative to those of **2** due to the local 6π aromatic nature of phenylene [8]. With this regard, a novel conjugative bridge to possess both moderate rigidity and effective conjugation has been desired to create novel conjugated expanded

◊ SPP full member in good standing.

*Correspondance to: Takayuki Tanaka, email: taka@kuchem.kyoto-u.ac.jp; tel.: +81 75-753-4007. fax: +81 75-753-3970.

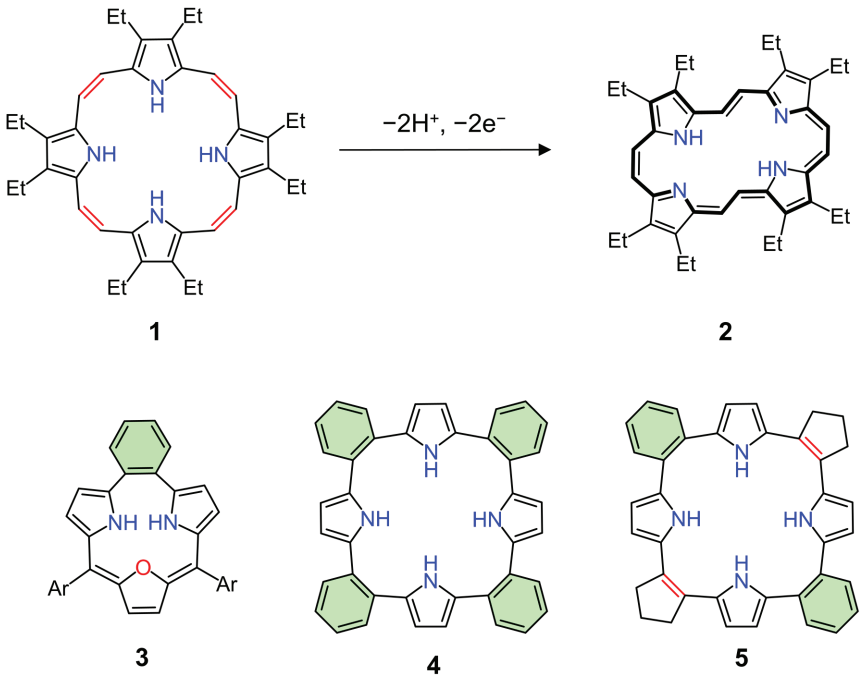

Fig. 1. (Top) β-Octaethylporphyrin(2.2.2.2) and (bottom) *ortho*-phenylene-bridged porphyrinoids. Ar = 3,5-di-*tert*-butylphenyl.

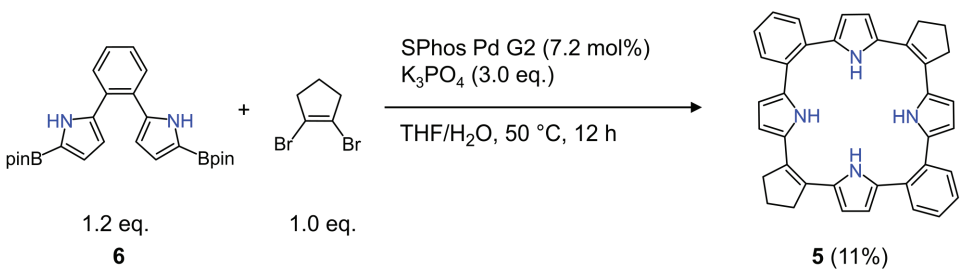

Scheme 1. Synthesis of *ortho*-phenylene-cyclopentene-bridged tetrapyrrole **5**.

porphyrinoids. Herein is a report on *ortho*-phenylene-cyclopentene-bridged tetrapyrrole **5**. The 1-cyclopentene bridge serves as a conjugative linker with defined *cis*-configuration, thereby causing an intermediate conjugation ability between those of **1** and **4**.

RESULTS AND DISCUSSION

As an advantageous feature over porphyrinoid synthesis, *ortho*-phenylene-bridged tetrapyrrole **4** can be synthesized by transition-metal catalyzed cross-coupling reaction [8, 9, 10]. Actually, **4** was prepared by the coupling of bis(*1H*-5-pincolatoborylpyrrol-2-yl)benzene (**6**) with 1,2-dibromobenzene in 10% yield [9]. By using the same reaction conditions, 1,2-dibromocyclopentene (**7**) [11] was coupled with **6** (Scheme 1). After purification by silica-gel column chromatography and gel permeation chromatography, cyclic tetrapyrrole **5** was obtained in 11% yield. High-resolution atmospheric-pressure-chemical-ionization time-of-flight (HR-APCI-TOF) mass spectrometry showed a molecular ion peak at *m/z* = 544.2615 (calcd. for $C_{38}H_{32}N_4$ *m/z* = 544.2621). The ^{1}H NMR spectrum of **5** in acetone-d_6 showed an NH peak at 9.55 ppm, two signals due to the phenylene protons at 7.50 and 7.24 ppm, two signals due to the pyrrolic β-protons at 6.43 and 6.24 ppm, and two signals due to the cyclopentene protons at 2.74 and 1.82 ppm (Fig. 2). Interestingly, the ^{1}H NMR spectral features were significantly changed at low temperature in CD_2Cl_2 (Fig. S6). All the peaks were coalesced at -40 °C, and new peaks appeared at -80 °C with a lower symmetry. This indicates that the dynamic motion is slower than the ^{1}H NMR time scale at low temperature.

Single crystals of **5** were obtained by slow diffusion of *n*-hexane into its chloroform solution (Fig. 3). Similarly to **2** and other *ortho*-phenylene-bridged cyclic pyrrole oligomers [8, 9, 10], **5** displays a twisted structure in the solid state. The average dihedral angle between the pyrrole and cyclopentene segments is 20.0°, while that between the pyrrole and phenylene segments is 38.5°

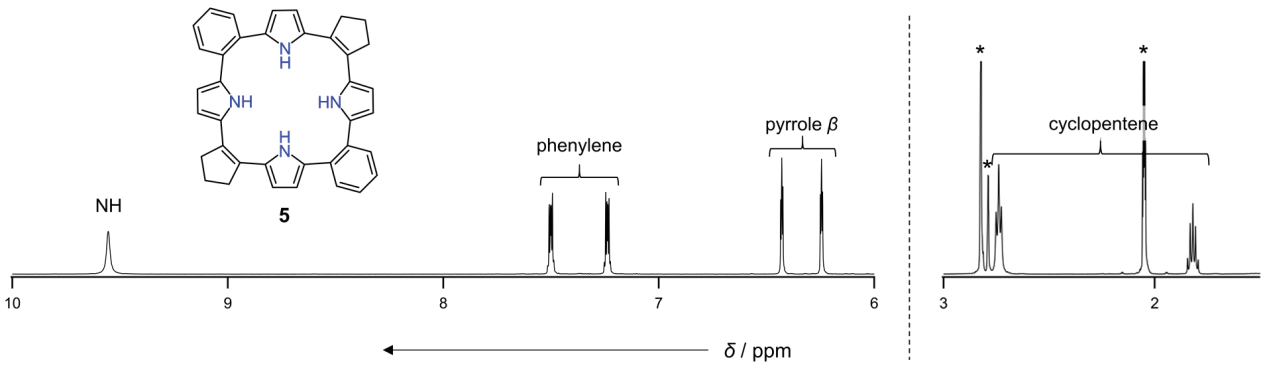

Fig. 2. ^{1}H NMR spectrum of **5** in acetone-d_6 at room temperature. Peaks with * are due to the residual solvents.

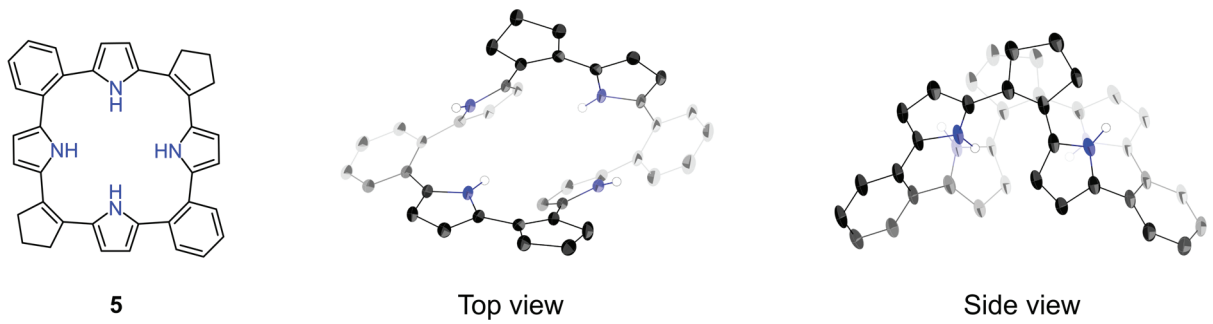

Fig. 3. X-Ray crystal structure of **5** with thermal ellipsoids at 50% probability. (Left) Top view and (right) side view. Solvent molecules and all hydrogen atoms except for those of NHs have been omitted for clarity.

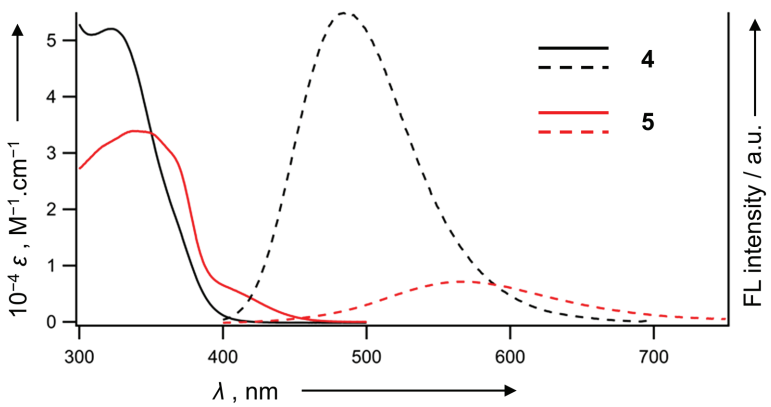

Fig. 4. UV-vis absorption (solid lines) and fluorescence (dashed lines) spectra of **4** (black) and **5** (red) in THF.

(Fig. S12). The difference may be imposed by the effective conjugation at the cyclopentene-bridge moiety as well as the smaller size of cyclopentene relative to phenylene. 3,4-Thienylene-bridged cyclic tetrapyrrole showed an even larger dihedral angle (46.6°), which suggests the importance of the conjugative interaction for smaller dihedral angles [12].

ortho-Phenylene-cyclopentene-bridged tetrapyrrole **5** exhibits an absorption band at 340 nm with a tail in the range of 390–500 nm in THF (Fig. 4). A weak and broad fluorescence band is observed at 568 nm with a smaller fluorescence quantum yield (Φ_F = 0.036) than that of **4** (Φ_F = 0.27) [8]. The fluorescence spectrum of **5** was also measured in PMMA (0.1 wt%) matrix, which displayed a peak at 553 nm (Φ_F = 0.15) (Fig. S15). The blue-shifted and enhanced emission is ascribed to the restricted dynamic motion in the S_1-state in the matrix. The solid state emission is even weaker (Φ_F = 0.024) and slightly red-shifted. The MO energy levels of **5** were calculated by DFT method (Fig. S18). The HOMO of **5** (-4.75 eV) is significantly destabilized by 0.5 eV relative to that of **4** (-5.27 eV). The cyclic voltammetry

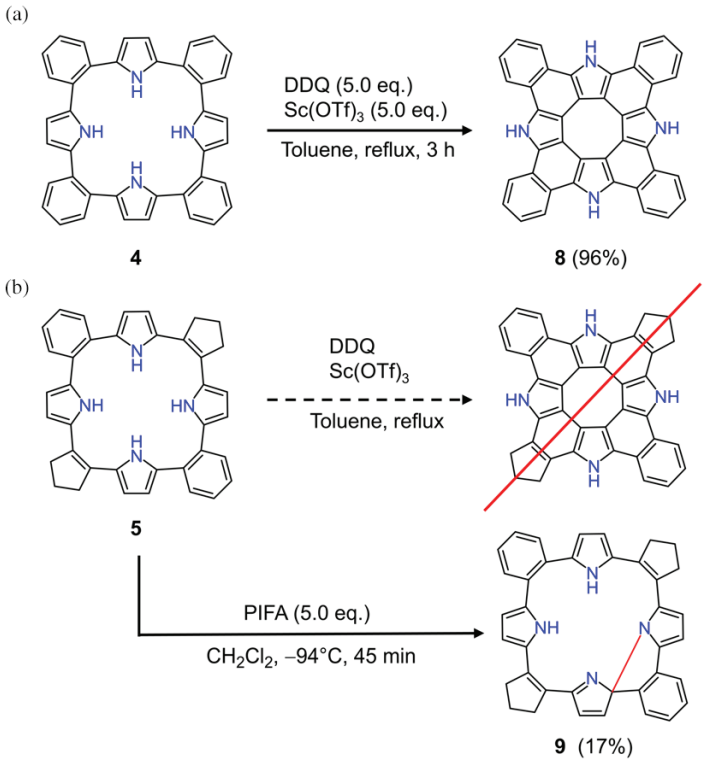

Scheme 2. (a) Fold-in synthesis of tetrabenzotetraaza[8]circulene (**8**). (b) An attempt to synthesize dibenzodicyclopentenotetraaza[8]circulene.

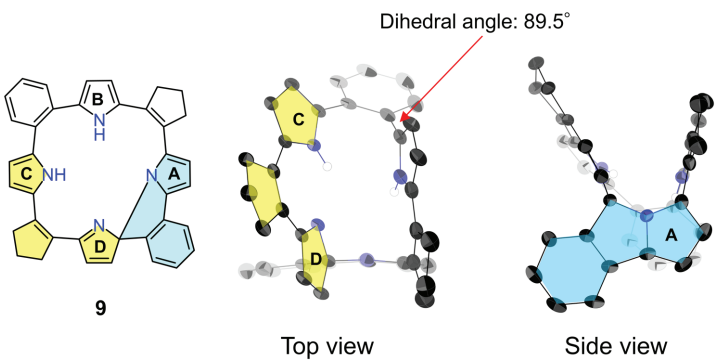

Fig. 5. X-Ray crystal structure of **9** with the thermal ellipsoids at 50% probability. (Left) Top view and (right) side view. All hydrogen atoms except for those of NHs have been omitted for clarity.

experiment confirmed two reversible oxidation waves of **5** at 0.075 and 0.203 V against ferrocene/ferrocenium ion couple in CH_2Cl_2 (Fig. S17). The first oxidation potential is cathodically shifted from that of **4** (0.176 V), being consistent with the results of DFT calculation. The LUMO of **5** (-1.42 eV) is stabilized, which resulted in the decreased HOMO–LUMO gap (3.3 eV), being consistent with the red-shifted absorption.

It had been previously reported that the "fold-in" oxidative fusion reaction of *ortho*-phenylene-bridged tetrapyrrole **4** afforded tetrabenzotetraaza[8]circulene **8** [8, 13]. The same transformation of **5** was examined by using 2,3-dichloro-5,6-dicyano-*p*-benzoquinone (DDQ) and scandium(III) trifluoromethanesulfonate ($Sc(OTf)_3$) under toluene reflux. However, only insoluble black solids were obtained. Then, **5** was oxidized with a milder oxidant, PIFA, at -94 °C [14]. After separation by silica-gel column chromatography, **9** was obtained as yellow solids in 17% yield. HR-APCI-TOF mass spectrometry showed a molecular ion peak of **9** at m/z = 542.2459 (calcd for $[C_{38}H_{30}N_4]^+$: 542.2465 $[M]^+$), indicating a loss of two hydrogens from **5**. Although the ^{1}H NMR spectral analysis of **9** is difficult to fully assign the structure, two NH peaks are observed at 12.68 and 7.97 ppm (Fig. S3). Finally, the X-ray diffraction analysis confirmed that a new N–C bond was formed between the pyrrolic nitrogen and the α-position of the adjacent pyrrole to form a spiro-conjugated pyrrolo[2,1-*a*]isoindole structure (Fig. 5) [15].

The fused moiety is highly planar, while the spiro-connected dipyrroethene unit (yellow-coloured area in Fig. 5) is also quite planar due to the intramolecular hydrogen bonding interaction between pyrroles C and D (Fig. S12). The UV-vis absorption spectrum of **9** exhibited a red-shifted absorption band in the range of 400–500 nm (Fig. S21). No fluorescence was observed in **9** in THF (Φ_F < 0.001). DFT calculation for **9** indicates a CT character between HOMO and LUMO, in which the HOMO is localized on the cyclopentenylpyrrole moiety (pyrrole B in Fig. 5) next to the pyrrolo[2,1-*a*]isoindole segment and the LUMO is localized on the 1,2-dipyrrolylcyclopentene moiety. Since the dihedral angle between the *ortho*-phenylene and pyrrole (B) segments is quite large (89.5°), the donor and acceptor segments are electronically separated, resulting in the fluorescence quenching presumably due to the intramolecular eletron transfer.

In summary, *ortho*-phenylene-cyclopentene-bridged tetrapyrrole **5** has been synthesized by a cross-coupling reaction. It showed a twisted structure with small dihedral angles between the pyrrole and cyclopentene moieties in the solid state. Oxidation of **5** with PIFA at low temperature resulted in the formation of unexpectedly N–C fused product **9** with a spiro connection at the α-position of the pyrrole segment. These results indicate that tetrapyrrole **5** represents a unique porphyrin(2.2.2.2) analogue and offers an opportunity to create novel polycyclic heteroaromatic molecules [16].

EXPERIMENTAL

General

Commercially available solvents and reagents were used without further purification unless otherwise noted. Dry tetrahydrofuran was obtained by passing through alumina under N_2 in a solvent purification system. Dry dichloromethane was distilled over CaH_2. SPhos Pd G2 was purchased from Sigma-Aldrich. Tripotassium phosphate was purchased from FUJIFILM Wako Pure Chemical Corporation. Bis(trifluoroacetoxy)iodobenznene (PIFA) was purchased from Tokyo Chemical Industry. The spectroscopic grade solvents were used for all the spectroscopic studies. Silica gel column chromatography was performed on Wakogel C-400. Thin-layer chromatography (TLC) was carried out on aluminum sheets coated with silica gel 60 F_{254} (Merck 5554). Recycling preparative GPC-HPLC was performed on a Japan Analytical Industry LaboACE LC-5060 equipped with JAIGEL-1HR (Φ20 mm, flow rate; 10 mL/min). UV-vis absorption spectra were recorded on a Shimadzu UV-3600 spectrometer. Fluorescence spectra were recorded on a Shimadzu RF-5300PC spectrometer. Absolute fluorescence quantum yields were determined on a HAMAMATSU C9920-02S. ^{1}H and ^{13}C NMR spectra were recorded on a JEOL ECA-600 spectrometer (operating as 600 MHz for ^{1}H and 151 MHz for ^{13}C) using the residual solvent as an internal reference for ^{1}H (δ = 2.05 ppm in acetone-d_6, 5.32 ppm in CD_2Cl_2) and ^{13}C (δ = 29.84 ppm in acetone-d_6). HR-APCI-TOF-MS was performed on a BRUKER micrOTOF model using positive mode. Redox potentials were measured on an ALS electrochemical analyzer model 612E.

Crystal Data

Single-crystal X-ray diffraction analysis data for **5** and **9** were collected at -180 °C with a Rigaku XtaLAB P200 by using graphite monochromated Cu-K_α radiation (λ = 1.54187 Å). The structures were solved by direct methods (SHELXS-2013/1 or SHELXT-2014/5) and refined with full-matrix least square technique (SHELXL-2014/7) [17].

Cyclopentene-benzene-bridged tetrapyrrole (5)

A 100 mL round-bottomed flask was charged with diborylated compound **6** (3.3 g, 7.2 mmol, 1.2 eq.), SPhos Pd G2 (310 mg, 0.43 mmol, 7.2 mol%), and tripotassium phosphate (3.8 g, 18 mmol, 3.0 eq.). The flask was evacuated and purged with argon three times. After the mixture was dissolved in dry THF (60 mL) and water (15 mL), 1,2-dibromocyclopentene **7** (0.71 mL, 6.0 mmol, 1.0 eq.) was added, and the reaction mixture was stirred at 50 °C for 12 h. After quenched with saturated aqueous ammonium chloride solution, the mixture was extracted with ethyl acetate three times, and the organic layer was washed with water and brine, dried over anhydrous sodium sulfate, and concentrated *in vacuo*. The residue was purified by silica gel column chromatography (dichloromethane/*n*-hexane = 3/2) and by recycling preparative GPC-HPLC with chloroform as an eluent to afford **5** (170 mg, 0.32 mmol, yield: 11%) as yellow solids.

Compound data for 5

^{1}H NMR (600 MH; acetone-d_6; RT) δ, ppm 9.55 (s, 4H; NH), 7.50 (dd, J_1 = 5.7, J_2 = 3.4 Hz, 4H; phenylene), 7.24 (dd, J_1 = 5.7, J_2 = 3.4 Hz, 4H; phenylene), 6.43 (t, J = 3.0 Hz, 4H; pyrrole β), 6.24 (t, J = 3.0 Hz, 4H; pyrrole β), 2.74 (t, J = 7.3 Hz, 8H; cyclopentene), and 1.82 (q, J = 7.3 Hz, 4H; cyclopentene); ^{13}C NMR (151 MHz; acetone-d_6; RT) δ, ppm 132.10, 131.77, 131.14, 130.41, 127.58, 124.52, 110.38, 110.09, 37.89, and 22.31. UV-vis (THF): λ_{max}, nm (ε [M^{-1} cm^{-1}]) = 285 (3.0×10^4) and 339 (3.4×10^4). HR APCI-TOF-MS (positive): *m*/*z* calcd for $[C_{38}H_{32}N_4]^+$: 544.2621 [M]$^+$; found: 544.2615.

PIFA oxidation of 5

A 50 mL round-bottomed flask was charged with 5 (30 mg, 55 μmol, 1.0 eq.). The flask was evacuated and purged with argon three times. After the mixture was dissolved in dry dichloromethane (30 mL), the reaction mixture was cooled at -94 °C. Then, PIFA (118 mg,

270 μmol, 5.0 eq.) was added, and the reaction mixture was kept at -94 °C for 10 mins. The reaction mixture was allowed to warm to ambient temperature. When fluorescence of the mixture was not observed, an excess amount of sodium borohydride and methanol was added, and the reactant was stirred for 30 mins at ambient temperature. The reaction mixture was poured into water and extracted with dichloromethane, and the combined organic layers were washed with water and brine, dried over anhydrous sodium sulfate, and concentrated *in vacuo*. The residue was purified by silica gel column chromatography (dichloromethane/*n*-hexane = 1/1) to afford 9 (5.0 mg, 9.2 μmol, yield: 17%) as yellow solids.

Compound data for 9

^{1}H NMR (600 MHz; acetone-d_6; RT) δ, ppm 12.68 (br s, 1H; NH), 7.97 (s, 1H; NH), 7.40 (d, J = 7.8 Hz, 1H; phenylene), 7.30 (m, 2H; phenylene), 7.26 (td, J_1 = 6.9, J_2 = 2.3 Hz, 1H; phenylene), 7.17 (m, 2H; phenylene), 7.14 (d, J = 4.8 Hz, 1H; pyrrole β), 7.01 (d, J = 4.8 Hz, 1H; pyrrole β), 6.92 (td, J_1 = 7.6, J_2 = 0.9 Hz, 1H; phenylene), 6.58 (d, J = 7.8 Hz, 1H; phenylene), 6.46 (d, J = 3.7 Hz, 1H; pyrrole β), 6.36 (dd, J_1 = 3.7, J_2 = 2.3 Hz, 1H; pyrrole β), 6.18 (d, J = 3.7 Hz, 1H; pyrrole β), 6.15 (dd, J_1 = 3.7, J_2 = 2.3 Hz, 1H; pyrrole β), 5.85 (t, J = 3.0 Hz, 1H; pyrrole β), 5.25 (t, J = 3.0 Hz, 1H; pyrrole β), 3.07 (m, 3H; cyclopentene), 2.90 (m, 1H; cyclopentene), 2.68 (m, 1H; cyclopentene), 2.62 (m, 2H; cyclopentene), 2.53 (m, 1H; cyclopentene), 1.95 (m, 3H; cyclopentene), and 1.86 (m, 1H; cyclopentene); ^{13}C NMR (151 MHz; acetone-d_6; RT) δ, ppm 171.38, 150.93, 142.60, 140.17, 138.77, 136.70, 135.03, 134.88, 134.44, 133.92, 132.95, 132.93, 132.38, 132.36, 130.79, 129.83, 129.46, 129.40, 127.66, 126.35, 122.40, 122.23, 120.90, 119.74, 114.47, 114.42, 113.03, 110.90, 110.83, 110.42, 108.53, 101.82, 40.75, 38.31, 38.06, 34.77, 23.45, and 22.46. UV-vis (THF): λ_{max}, nm (ε [M^{-1} cm^{-1}]) = 286 (3.6×10^4), and 443 (8.7×10^3). HR APCI-TOF-MS (positive): *m*/*z* calcd for $[C_{38}H_{30}N_4]^+$: 542.2465 $[M]^+$; found: 542.2459.

Acknowledgments

This work was supported by JSPS KAKENHI Grant Numbers (JP18H03910 and JP20K05463). The authors acknowledge Prof. Dr. H. Yorimitsu (Kyoto University) for HR-APCI-TOF MS measurements.

Supporting information

Figures of NMR spectra, mass spectra, UV-vis and fluorescence spectra, cyclic voltammetry, DFT calculation and crystallographic data are given in the supplementary material. This material is available free of charge *via* the Internet at https://www.worldscientific.com/doi/suppl/10.1142/S1088424621500553.

Crystallographic data have been deposited at the Cambridge Crystallographic Data Centre (CCDC) under numbers CCDC-2072348 (**5**) and -2072349 (**9**). Copies can be obtained on request, free of charge, *via* http://www.ccdc.cam.ac.uk/data_request/cif or from the Cambridge Crystallographic Data Centre, 12 Union Road, Cambridge CB2 1EZ, UK (fax: +44 1223-336-033 or email: deposit@ccdc.cam.ac.uk).

REFERENCES

1. (a) Berger RA and LeGoff E. *Tetrahedron Lett*. 1978; **19**: 4225–4228. (b) Gosmann M and Franck B. *Angew. Chem. Int. Ed. Engl.* 1986; **25**: 1100–1101. (c) Franck B and Nonn A. *Angew. Chem. Int. Ed. Engl.* 1995; **34**: 1795–1811. (d) Eickmeier C and Franck B. *Angew. Chem. Int. Ed. Engl.* 1997; **36**: 2213–2215.
2. (a) Roznyatovskiy V, Lynch V and Sessler JL. *Org. Lett.* 2010; **12**: 4424–4427. (b) Sarma T, Panda PK, Anusha PT and Rao SV. *Org. Lett.* 2011; **13**: 188–191. (c) Ganapathi E, Chatterjee T and Ravikanth M. *Eur. J. Org. Chem.* 2014; 6701–6706. (d) Oohora K, Ogawa A, Fukuda T, Onoda A, Hasegawa JY and Hayashi T. *Angew. Chem. Int. Ed.* 2015; **54**: 6227–6230. (e) Kuzuhara D, Sakaguchi M, Furukawa W, Okabe T, Aratani N and Yamada H. *Molecules* 2017; **22**: 908. (f) Xu N, Ono T and Hisaeda Y. *Chem. Eur. J.* 2019; **25**: 11680–11687. (g) Ono T, Xu N, Koga D, Ideo T, Sugimoto M and Hisaeda Y. *RSC Adv.* 2018; **8**: 39269–39273.
3. (a) Waluk J. *Chem. Rev.* 2017; **117**: 2447–2480. (b) Anguera G and Sánchez-García D. *Chem. Rev.* 2017; **117**: 2481–2516. (c) Sarma T and Pand PK. *Chem. Rev.* 2017; **117**: 2785–2838. (d) Szyszko B, Białek MJ, Pacholska-Dudziak E and Latos-Grażyński L. *Chem. Rev*. 2017; **117**: 2839–2909. (e) Setsune J-i. *Chem. Rev.* 2017; **117**: 3044–3101. (f) Kuzuhara D and Yamada H. *Synlett* 2020; **31**: in press (DOI:10.1055/s-0040-1705979)
4. (a) Szydlo F, Andrioletti B and Rose E. *Org. Lett.* 2006; **8**: 2345–2348. (b) Umetani M, Tanaka T, Kim T, Kim D and Osuka A. *Angew. Chem. Int. Ed.* 2016; **55**: 8095–8099. (c) Kuzuhara D, Furukawa W, Kitashiro A, Aratani N and Yamada H. *Chem. Eur. J.* 2016; **22**: 10671–10678. (d) Kuzuhara D, Furukawa W, Aratani N and Yamada H. *J. Porphyrins Phthalocyanines* 2020; **24**: 489–497.
5. (a) Jux N, Koch P, Schmickler H, Lex J and Vogel E. *Angew. Chem. Int. Ed.* 1990; **29**: 1385–1387. (b) Vogel E, Jux N, Rodriguez–Val E, Lex J and Schmickler H. *Angew. Chem. Int. Ed.* 1990; **29**: 1387–1390.
6. Rana A, Lee S, Kim D, Panda P. K. *Chem. Eur. J.* 2015; **21**: 12129–12135.

7. (a) Pawlicki M, Hurej K, Szterenberg L and Latos-Grażyński L. *Angew. Chem. Int. Ed.* 2014; **53**: 2992–2996. (b) Pawlicki M, Garbicz M, Szterenberg L and Latos-Grażyński L. *Angew. Chem. Int. Ed.* 2015; **54**: 1906–1909. (c) Bartkowski K and Pawlicki M. *Angew. Chem. Int. Ed.* 2021; **60**: 9063–9070.
8. Chen F, Hong Y, Shimizu S, Kim D, Tanaka T, Osuka A. *Angew. Chem. Int. Ed.* 2015; **54**: 10639–10642.
9. Morimoto Y, Chen F, Matsuo Y, Kise K, Tanaka T, Osuka A, *Chem Asian J*. 2021; **16**: 648–655.
10. (a) Chen F, Tanaka T, Hong Y, Kim W, Kim D and Osuka A. *Chem. Eur. J.* 2016; **22**: 10597–10606. (b) Chen F, Kim J, Matsuo Y, Hong Y, Kim D, Tanaka T and Osuka A. *Asian J. Org. Chem.* 2019; **8**: 994–1000.
11. Pijper TC, Kudernac T, Browne WR, Feringa BL. *J. Phys. Chem. C* 2013; **117**: 34, 17623–17632.
12. Kise K, Chen F, Kato K, Tanaka T and Osuka A. *Chem. Lett.* 2017; **46**: 1319–1322.
13. (a) Hensel T, Anderson NN, Plesner M and Pittelkow M. *Synlett* 2016; **27**: 498–525. (b) Miyake Y and Shinokubo H. *Chem. Commun.* 2020; **56**: 15605–15614.
14. (a) Chen F, Tanaka T, Mori T and Osuka A. *Chem. Eur. J.* 2018; **24**: 7489–7497. (b) Matsuo Y, Tanaka T and Osuka A. *Chem. Eur. J.* 2020; **26**: 8144–8152.
15. (a) Mitsumori T, Bendikov M, Dautel O, Wudl F, Shioya T, Sato H and Sato Y. *J. Am. Chem. Soc.* 2004; **126**: 16793–16803. (b) Yi C, Blum C, Liu SX, Frei G, Neels A, Stoeckli-Evans H, Leutwyler S and Decurtins S. *Tetrahedron* 2008; **64**: 9437–9441. (c) Yang DT, Radtke J, Mellerup SK, Yuan K, Wang X, Wagner M and Wang S. *Org. Lett.* 2015; **17**: 1114–1117. (d) Kuzuhara D, Miyake S, Moriyama H, Tamura Y, Aratani N and Yamada H. *Tetrahedron Lett.* 2015; **56**: 5564–5567. (e) Zheng W, Zhao Y, Zhuang WH, Wu JJ, Wang FZ, Li CH and Zuo JL. *Angew. Chem. Int. Ed.* 2018; **57**, 15384–15389. (f) Zeng C, Yuan K, Wang N, Peng T, Wu G and Wang S. *Chem. Sci*. 2019; **10**: 1724–1734. (g) Chintawar CC, Mane MV, Tathe AG, Biswas S, Patil NT. *Org. Lett*. 2019; **21**: 7109–7113.
16. Stępień M, Gońka E, Żyła M and Sprutta N. *Chem. Rev.* 2017; **117**: 3479–3716.
17. SHELXS-2013/1 and SHELXT-2014/5, Program for the Refinement of Crystal Structures from Diffraction Data, University of Göttingen, Göttingen (Germany); Sheldrick GM and Schneider TR. *Methods Enzymol.* 1997; **277**: 319–343.